ELSEVIER

Fusion Engineering and Design 65 (2003) 303–322

Fusion Engineering and Design

www.elsevier.com/locate/fusengdes

The toroidal field coil design for ARIES-ST

W. Reiersen *, F. Dahlgren, H.-M. Fan, C. Neumeyer, I. Zatz, The ARIES Team

Princeton Plasma Physics Laboratory, Princeton University, James Forrestal Campus, P.O. Box 451, Princeton, NJ 08543, USA

Abstract

An evolutionary process was used to develop the toroidal field (TF) coil design for the ARIES-spherical torus (ST). Design considerations included fabricability, assembly, maintenance, energy efficiency, and structural robustness. Design options were identified early in the process. Trade studies were carried out to identify preferred choices. Design points were re-optimized based on the design choices in the TF and other systems. An attractive design for the ARIES-ST TF coil system evolved. This design addresses a number of the concerns (complexity) and criticisms (high cost, high recirculating power) of fusion. It does this by: applying advanced, but available laser forming and spray casting techniques for manufacturing the TF coil system; adopting a simple single turn TF coil system to make assembly and maintenance much easier. The single turn design avoids the necessity of using the insulation as a structural component of the TF coils, and hence, is much more robust than multi-turn designs; using a high conductivity copper alloy and modest current densities to keep the recirculating power modest.
© 2002 Elsevier Science B.V. All rights reserved.

Keywords: ARIES-ST; Toroidal field; Embrittlement

1. Introduction

The goal of this study was to develop an attractive toroidal field (TF) coil configuration for a spherical torus (ST) power plant. The TF system must be capable of providing a field of 2.14 T at a major radius of 3.2 m and be compatible with the overall maintenance concepts. Trade studies conducted to choose between key design options are described in Section 2. A design description of the TF coil and power supply systems is provided in Section 3. System performance is described in Section 4. Conclusions of the study are provided in Section 5.

2. Design options

2.1. Single or multi-turn TF coils

The choice of a single turn or multi-turn TF is the most critical choice to be made in developing a TF system for a ST. A single turn configuration has some marked advantages:

- No turn-to-turn electrical insulation is required. This results in an improved packing fraction, reduced shielding requirements, elimination of

* Corresponding author. Tel.: +1-609-243-2479
E-mail address: reiersen@pppl.gov (W. Reiersen).

0920-3796/02/$ - see front matter © 2002 Elsevier Science B.V. All rights reserved.
PII: S0920-3796(02)00308-3

concerns about turn-to-turn electrical breakdown, and a stronger mechanical design for the centerpost due to its monolithic construction;
- Operating voltages are much lower;
- Changes in electrical conductivity over time are gracefully accommodated by natural current redistribution within the centerpost.

A multi-turn configuration also has advantages:

- Power supplies and buses are in smaller units. Joule losses in the power supplies and buses are lower due to dramatically reduced coil currents (in the range of tens to hundreds of kilo-amperes in a multi-turn TF compared to tens of mega-amperes for a single turn TF); and
- Compatibility with conventional coil fabrication techniques.

The large conductor currents in the single turn configuration, while formidable, do not appear intractable from a power supply standpoint. A scheme for providing a very high current (multi-mega-ampere) power supply has been developed. The scheme uses a large number of diode rectifiers connected in parallel to provide current to the TF load.

A single turn centerpost configuration can carry more current than a multi-turn configuration of the same radius because of its higher packing fraction (no insulation, flexible conductor geometry) and reduced shielding requirement (no insulation). Thus, the single turn configuration provides an upper bound on how economically attractive a spherical tokamak (ST) power plant might be. This is the reason it was adopted for the reference design.

2.2. Centerpost material selection

Nearly pure copper alloys (e.g., C102-OFHC Cu, C107-Oxygen free with Ag, and C110-Electrolytic Tough Pitch) were commonly the conductors of choice for early normal (i.e., non-superconducting) tokamaks. Although not as strong as other copper alloys, they provided adequate strength in addition to outstanding electrical and thermal characteristics and were readily available at reasonable cost. For power plant applications, the requirements are somewhat broader:

- Adequate mechanical properties (strength and ductility) at end of life;
- Adequate physical properties (swelling, electrical conductivity, thermal conductivity, and activation) at end of life; and
- Availability in required shapes and sizes.

The centerpost, unless very well shielded, will be subject to high radiation doses. Potential radiation effects in the centerpost include embrittlement, activation, void swelling, irradiation creep, decrease in electrical and thermal conductivity, and radiation hardening.

2.2.1. Mechanical properties

With the exception of precipitation heat-treated or dispersion strengthened (DS) copper alloys, copper must be cold worked to achieve high strength. This is relatively easy to do with plates (which are rolled) or wires and rods (which are drawn), but would be extremely difficult, if not impossible to perform with uniform properties on a large assembly such as the centerpost. Furthermore some of the ST cooling options, as discussed in the following sections, result in centerpost temperatures in ranges that would anneal (soften) pure copper and many of its alloys. Precipitation heat-treated and DS copper alloys are favored for these reasons.

Copper alloys are available that provide higher strength (especially at elevated temperatures) but with reduced electrical and thermal conductivity. For this study, two alloys were considered—the precipitation hardened (PH) alloy CuCrZr (with a nominal composition of Cu-0.65%Cr-0.15%Zr) and the DS alloy Glidcop AL-15 (with a nominal composition of Cu-0.15%Al as oxide particles 0.28%Al_2O_3). These alloys represent two different classes of materials. Both have been well characterized in a radiation environment as a result of extensive testing conducted on the international thermonuclear experimental reactor (ITER) project. A summary of the material characteristics for Glidcop AL-15 and CuCrZr is provided in Table 1.

Table 1
Material characteristics for Glidcop AL-15 and CuCrZr

Property	Glidcop AL-15	CuCrZr
Condition	As wrought	Solutionized and aged
Electrical conductivity	89% IACS. Degrades under irradiation, primarily due to Cu transmuting to Ni and Zn [5]	80% IACS [5]. Degrades under irradiation, primarily due to Cu transmuting to Ni and Zn [5]
Radiation-induced swelling	Not susceptible to swelling low temperature (< 150 °C)	Not susceptible to swelling low temperature (< 150 °C)
Strength	Room temperature, unirradiated (AL-25): TYS ~ 340 MPa, UTS ~ 410 MPa [13] Radiation hardens (+150 MPa) above 0.1 dpa at low temperature (< 150 °C) [3]	Room temperature, unirradiated: TYS ~ 435 MPa, UTS ~ 475 MPa [13] Radiation hardens (+150 MPa) above 0.1 dpa at low temperature (< 150 °C) [3] Maximum TYS following brazing or welding 350 MPa [5]
Fatigue	Room temperature, unirradiated—maximum stress at 10^5 cycles is 300 MPa [5]	Room temperature, unirradiated—maximum stress at 10^5 cycles is 250 MPa [5]
Creep	Low ($< 10^{-8}$/s) at stress levels below 250 MPa and temperatures below 300 °C [5]	Low ($< 10^{-8}$/s) at stress levels below 250 MPa and temperatures below 300 °C [5]
Fracture toughness	Drops markedly with temperature between 25 and 250 °C [12]	Drops slightly with temperature between 25 and 250 °C [12] Better than Glidcop AL-15 before and after irradiation [7]
Embrittlement	Drop in uniform elongation to 0.1–1% above 0.01 dpa [3]	Drop in uniform elongation to 0.1–1% above 0.01 dpa [3]
Activation	Includes 0.28% Al_2O_3, not a differentiating factor in the WDR	Includes 0.65% Cr and 0.10% Zr, not a differentiating factor in the WDR
Fabricability	Normally produced by powder metallurgy techniques, consolidated by hot extrusion or hot rolling Feasibility of laser forming appears unlikely—extremely difficult to do with DS copper as the Al_2O_3 particles would tend to redistribute during the melting process [7]	Can be cast and heat-treated Compatible with laser forming technique if the material can be properly heat-treated either during or after the deposition and shaping process [7]

Both materials exhibit very good strength (greater than 300 MPa TYS and 400 MPa UTS) at room temperature in the unirradiated condition. Because of the complexity of manufacturing the centerpost, no cold working was assumed for comparing material properties. The electrical conductivity of Glidcop AL-15 is approximately 90% IACS at room temperature, significantly higher than CuCrZr with an electrical conductivity of approximately 80%.

Irradiation at temperatures below 150 °C causes hardening in pure copper and PH and DS copper alloys. Hardening resulting from low temperature irradiation is accompanied by severe embrittlement [1] in PH and DS alloys. The uniform elongation generally decreases to less than 1% even at doses as low as 0.01–0.1 dpa. The expected peak dose at the centerpost after 1 full power year (FPY) of operation is 12 dpa [2]. Thus, these materials, if used in the centerpost and irradiated at low temperatures (< 150 °C), would be brittle.

At temperatures greater than 150 °C, PH and DS copper alloys remain ductile, with irradiated elongations in the range of 50–90% of the unirradiated values [3]. However, the Joule losses in the centerpost would be elevated due to the increase in electrical resistivity with temperature. The increase in electrical resistivity for OFHC Cu, Glidcop AL-15, and CuCrZr with temperature is

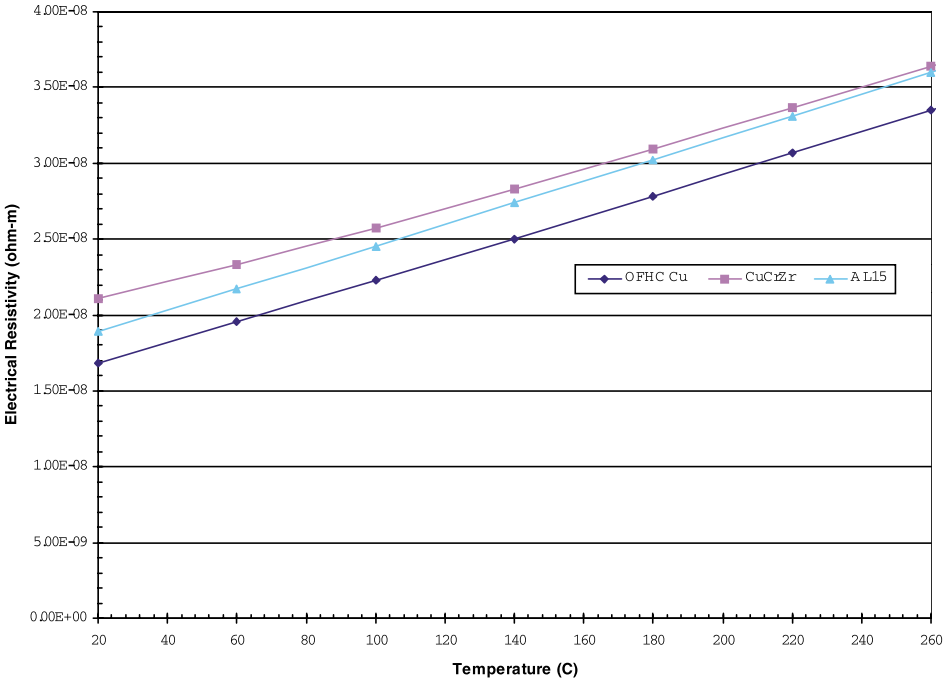

Fig. 1. Resistivity of OFHC Cu, Glidcop AL-15, and CuCrZr.

shown in Fig. 1. For CuCrZr, the electrical resistivity increases by 50% when the temperature is increased from 20 to 190 °C. To avoid the higher Joule losses associated with high conductor temperatures, the inlet temperature for the reference design was set at 30 °C, slightly above ambient temperature. Peak temperatures were below 100 °C. Brittle material allowables were used in evaluating the design. At temperatures less than 150 °C with stress levels below 250 MPa, creep is not expected to be an issue. Likewise, swelling should not be significant at temperatures less than 150 °C [1].

2.2.2. Physical properties

All copper alloys will be subject to transmutations that decrease the electrical and thermal conductivity and elevate the waste disposal rating (WDR). One of the requirements for ARIES-ST is to limit the WDR of the TF coils to Class C waste (low-level waste qualified for shallow land burial). With a 20-cm helium-cooled, ferritic steel shield, the design life of the centerpost in ARIES-ST is 3 FPY using 10CFR61 limits and 6 FPY using Fetter limits [4]. The design life of the ferritic shield structures surrounding the plasma is 3 FPY so the centerpost would have to be replaced either every replacement or every second replacement of the ferritic steel structures, depending on which limits were used, in order to satisfy WDR requirements. The 10CFR61 WDR is determined mainly from the long-lived isotopes produced from the Cu itself (^{63}Ni), not from the alloying elements. The Fetter WDR is determined mainly from ^{108m}Ag, produced from silver impurities that are not presently controlled in the material specifications. In either case, the WDR does not appear to be a differentiating factor in selecting the conductor material.

A thinner shield would require more frequent replacement of the centerpost based on WDR considerations and result in more nuclear heating and radiation damage in the centerpost. The nuclear heating in the centerpost with a 20-cm shield is approximately 164 MW [2]. This energy is not recovered because of the low operating tem-

perature in the centerpost. The peak radiation damage in the centerpost is 12 dpa/FPY. After 6 FPY, the peak radiation damage would be 72 dpa.

The dominant transmutation products affecting the electrical and thermal conductivity are nickel and zinc [5]. In addition, there is a decrease in conductivity due to radiation damage. This component appears to saturate at very low radiation fluence whereas the component due to transmutations is proportional to the radiation fluence. At the fluence levels calculated in the centerpost at the end of its useful life, the decrease in conductivity would be predominantly due to transmutations.

Calculations were performed to assess the increase in the electrical resistance of the centerpost over time due to transmutations. The results are shown in Fig. 2 and Fig. 3. Initially, the current distribution in the centerpost is nearly uniform. The decrease near the outer edge is due to the higher temperature resulting from nuclear heating. Over time, the current density near the outer edge drops dramatically due to the local increase in electrical resistivity. The current density in the center of the centerpost increases to keep the total current constant. The net effect, as shown in Fig. 3, is that the resistance of the centerpost increases more than 4% per FPY. After 3 FPY, the centerpost resistance would increase by approximately 12.5%. This represents a decrease in net electrical power of approximately 33 MW. After 6 FPY, the centerpost resistance would increase by approximately 23%, resulting in a decrease in net electrical power of 58 MW. Plant economics appear to favor

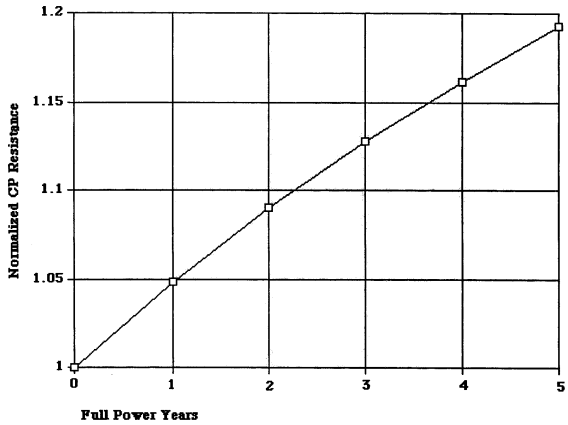

Fig. 3. Increase in centerpost resistance as a function of time.

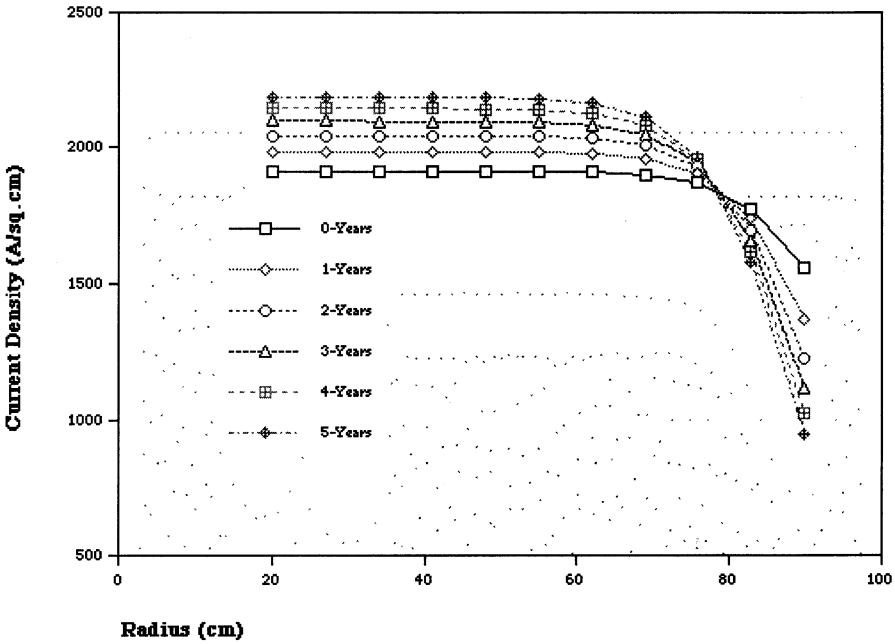

Fig. 2. Current density redistribution with accumulated neutron damage.

replacing the centerpost every 3 FPY (corresponding to the replacement time for the plasma facing ferritic steel structures) because the centerpost is relatively inexpensive ($7M), although WDR considerations might allow a 6 FPY replacement time.

2.2.3. Fabricability

The economics of fusion power are driven by the capital cost of the plant. The cost of the magnet systems has traditionally been a large element in the overall capital cost. For ARIES-ST, a study of low cost fabrication options for the TF system was performed by the Boeing Company with support from the AeroMet Corporation [6]. Two low cost fabrication methods were identified—laser forming for the centerpost and spray casting for the TF outer shell. The cost of laser forming the centerpost from powdered copper was estimated to be approximately $8/kg. The cost of spray casting the outer shell from molten aluminum was approximately $4/kg. Applying these methods substantially lowers the capital cost of the plant.

Use of the laser forming technique for fabricating the centerpost may be a differentiating factor in selecting the best copper alloy. For Glidcop AL-15, a copper alloy which is DS with Al_2O_3, it would be difficult to use the current technology for laser forming as the Al_2O_3 particles would tend to redistribute during the melting process. Using a PH alloy such as CuCrZr may be feasible if the material could be properly heat-treated either during or after the deposition and shaping process [7].

Throughout most of the ARIES-ST study, Glidcop AL-15 properties were assumed for the centerpost because of its superior electrical conductivity. Following the fabrication study, CuCrZr properties were adopted because it appeared more feasible to fabricate the centerpost using laser forming with this material. However, from a broad perspective, these two alloys represent a class of materials (high conductivity, high strength copper alloys, with good fabrication characteristics) that appears able to meet the requirements for the centerpost of a low aspect ratio, tokamak power plant.

2.3. Cooling options

Early in the design of the ARIES-ST TF coil system, a trade study was conducted to assess candidate cooling options. Several cooling options were identified for evaluation:

- Liquid lithium at elevated temperature (200 °C inlet)
- Water at elevated temperature (180 °C inlet)
- Water at ambient temperature (35 °C inlet)
- Liquid nitrogen (LN_2) (80 K inlet)
- Gaseous helium (30 K inlet)
- Gaseous helium (10 K inlet)

A simple power flow model (Fig. 4) for the plant was constructed for the purpose of evaluating these options. Organic coolants, commonly used in process industries in elevated temperature applications, were not modeled because of their rapid degradation in a high radiation environment. A minimum shield thickness of 20 cm was imposed based on WDR considerations. For the cryogen-cooled options, the shield thickness was chosen to minimize the heat load to the refrigerator. An increased shield thickness reduces the nuclear heating at the expense of increased Joule heating. All options are limited to an inlet pressure of 3.47 MPa (500 psi). Coolant velocities were limited to 20 m/s for gaseous helium and 10 m/s for all other coolants.

Liquid metal cooling was first considered in the context of an integrated blanket coil (IBC). In the IBC concept, liquid lithium serves as a breeding material, a conductor, and a coolant. Calculations showed that a pure liquid lithium system is unattractive because of excessive Joule losses. Using the liquid metal as a coolant inside a copper conductor can reduce these losses. Glidcop AL-15 was assumed as the conductor material because of the need to operate at temperatures above the melting point of lithium (180 °C). A thin steel sleeve is required between the lithium and the conductor because of material compatibility issues. An electrically insulating coating must be applied to the inside of the steel sleeve to reduce MHD pressure drops to manageable levels. The option would only be interesting if water cooling

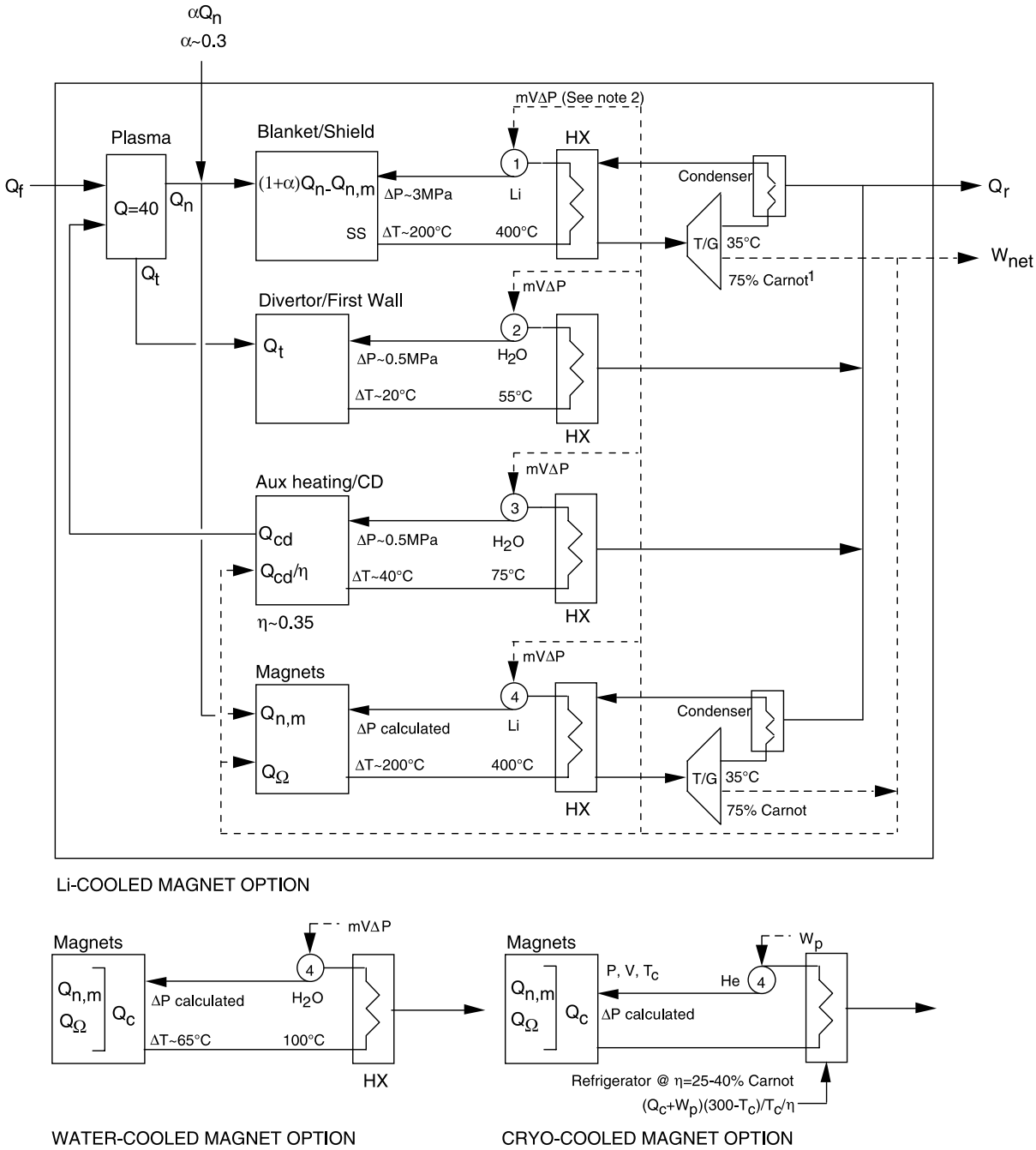

[1] All power conversion cycles are assumed to operate at 75% of the Carnot efficiency, i.e. $W/Q_a=0.75(T_a-T_r)/T_a$

[2] All pumps are assumed to be 75% efficient

Fig. 4. Power flow model for cooling options study.

was not compatible with the blanket or first wall cooling scheme. The maximum conductor temperature is necessarily high (290 °C), owing to the high inlet temperature (200 °C) and high temperature drop across the conductor, steel sleeve, and insulator. Radiation embrittlement should not be a concern in this temperature range but loss of fracture toughness is a concern. Joule losses are 70% higher than in a water-cooled coil because of the higher operating temperature and higher coolant fraction. Even with optimistic assumptions for energy recovery, the higher Joule losses are only marginally offset. In addition, the engineering difficulties associated with the liquid lithium coolant are severe.

Embrittlement due to irradiation at low temperatures (< 150 °C) and loss of fracture toughness at elevated temperatures and in a high radiation environment (data at 250 °C) are radiation effects relevant to Glidcop AL-15. Water is a candidate coolant that can be used to keep the conductor within a 150–230 °C temperature range without exceeding reasonable pressures or flow velocities. However, Joule losses will be about 50% higher than when the conductor is cooled with ambient water. Thus, the ambient water option is preferred over the warm water option if stresses in the centerpost can be kept within allowable limits for brittle materials.

A fourth option is to use copper operating in a temperature range appropriate for LN_2 cooling (80–110 K). The resistivity of copper drops substantially from room temperature to 80 K, in the ratio of approximately 7.7:1, so there is an incentive for operating at lower temperatures. However, in order to minimize the heat load to the refrigerator, the shield thickness has to be increased from 20 to 44 cm. The peak TF field increases to 8.8 T and the conductor current density to 2.1 kA/cm^2. The Joule heating in the centerpost drops from 300 to 76 MW, even with the smaller centerpost radius. The nuclear heating in the centerpost drops from 158 to 35 MW. Nevertheless, the net electric power drops to 423 MW (far less then the nominal 1000 MW for the ambient water-cooled option) because of the poor thermodynamic efficiency in removing heat at 80 K, approximately 7 W per watt removed.

Another option is to use copper operating in the temperature range of 30–50 K using gaseous helium. The resistivity of copper drops substantially from room temperature to 30 K, in the ratio of approximately 100:1, so there is incentive for operating at temperatures even lower than 80 K. In order to minimize the heat load to the refrigerator, the shield thickness has to be increased to 66 cm. The peak TF field increases to 11.5 T and the conductor current density to 4.1 kA/cm^2. The Joule heating in the centerpost drops to 15 MW. The nuclear heating in the centerpost drops to 9 MW. Nevertheless, the net electric power is still only 388 MW because of the very poor thermodynamic efficiency in removing heat at 30 K, approximately 37 W per watt removed.

The resistivity of copper becomes independent of temperature at temperatures below ~ 20 K. Copper also exhibits a strong magneto-resistance. For temperatures less than 20 K, the magneto-resistance for high conductivity copper (RRR > 100) is dominant above 4 T. Aluminum exhibits a much weaker magneto-resistance than copper that saturates with increasing field. Thus, high purity aluminum is often proposed as a conductor in very low temperature (< 20 K), high field applications. Using high purity aluminum conductor in the temperature range of 10–20 K appears optimal based on a minimization of the product of the resistivity and the Carnot work ($W_c \sim (T_h - T_c)/T_c$ in W/W). The average resistivity is assumed to be 0.008 μΩ cm with an average field of 9.7 T. This is lower than RT copper by the ratio of 215:1. The zero field resistivity for this high purity (99.999% pure) aluminum is 0.0009 μΩ cm at 15 K and has a RRR exceeding 5000 at 4 K. The high purity aluminum conductor can be cooled with gaseous helium. In order to minimize the heat load to the refrigerator, the shield thickness has to be increased to 80 cm. The peak TF field increases to 14.5 T and the conductor current density to 5.5 kA/cm^2. The Joule heating in the centerpost drops to 5.0 MW. The nuclear heating in the centerpost drops to 3.8 MW. Nevertheless, the net electric is still a meager 57 MW because of the extremely poor thermodynamic efficiency in removing heat at 10 K, approximately 119 W per watt removed. The bottom line is that the cryogen-cooled options

do not appear to offer any improvement over the water-cooled and Li-cooled options based on thermodynamic efficiencies for the design point used in this study. Cryogen-cooled options also appear to be much more complex.

The conclusion of the study of alternate cooling options was that none of the options, which ranged from gaseous helium at 10 K to liquid lithium at 200 °C, appeared superior to ambient water cooling when thermodynamic efficiency and design simplicity are taken into account.

3. Design description

3.1. TF coil system design

The configuration concept for the single turn coil system adopted for ARIES-ST is illustrated in Fig. 5. The configuration features a tall centerpost that is oriented along the major axis of the machine. The centerpost is connected to an outer shell that surrounds the first wall, blanket, shield, divertors, and PF coils. The TF system provides the primary vacuum boundary for the machine.

The centerpost is designed to be physically separable from the power core assembly. The bottom portion of the centerpost is a thick cylinder. It is electrically connected to the outer shell by sliding joints. The centerpost and outer shell are keyed together in this location, permitting relative motion radially and vertically while keeping them registered toroidally. Numerous concepts for sliding electrical contacts have been developed, tested, and even deployed for fusion applications. These concepts include; Feltmetal pads (used on C-Mod and proposed on MAST), Multilam sliding contacts [8], and spring-loaded, in-line contacts [9]. Liquid metal joints have also been considered. For this study, a sliding joint utilizing Feltmetal pads was assumed in developing the configuration concept. In addition to easing assembly and maintenance, the sliding joints significantly reduce axial stresses in the centerpost. This is a very important feature, since the centerpost will be come embrittled during operation.

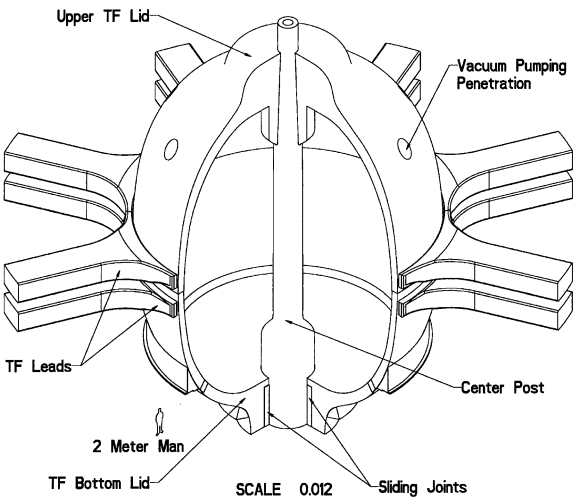

Fig. 5. Isometric view of TF coil system.

The centerpost transitions from a large diameter (3.2 m) cylinder at the bottom to a smaller diameter (1.8 m) cylinder between the upper and lower divertors. This is the region of high current density, accounting for most of the Joule losses. Flaring the centerpost on top as it is on the bottom would have trapped the centerpost with the power core assembly. Instead, the flaring is incorporated into the upper section of the outer shell. The centerpost has a conical shape above the upper divertor assembly where it is pulled against a mating surface in the outer shell for electrical continuity. Gravity support of the centerpost and the preload for the required contact pressure between the upper part of the centerpost and outer shell are provided where the centerpost penetrates the top of the outer shell. This arrangement allows the centerpost to be removed either without disturbing the power core assembly or as part of the power core assembly, as shown in Fig. 6. It also minimizes Joule losses by restricting the region of high current density to the cylindrical section between the upper and lower divertors. Since the TF provides the primary vacuum boundary, there are bellows connections above and below the outer shell where the centerpost penetrates the outer shell to provide vacuum seals.

The outer shell is segmented into three pieces, as shown in Fig. 5. The lower section of the outer shell provides the gravity support for the power

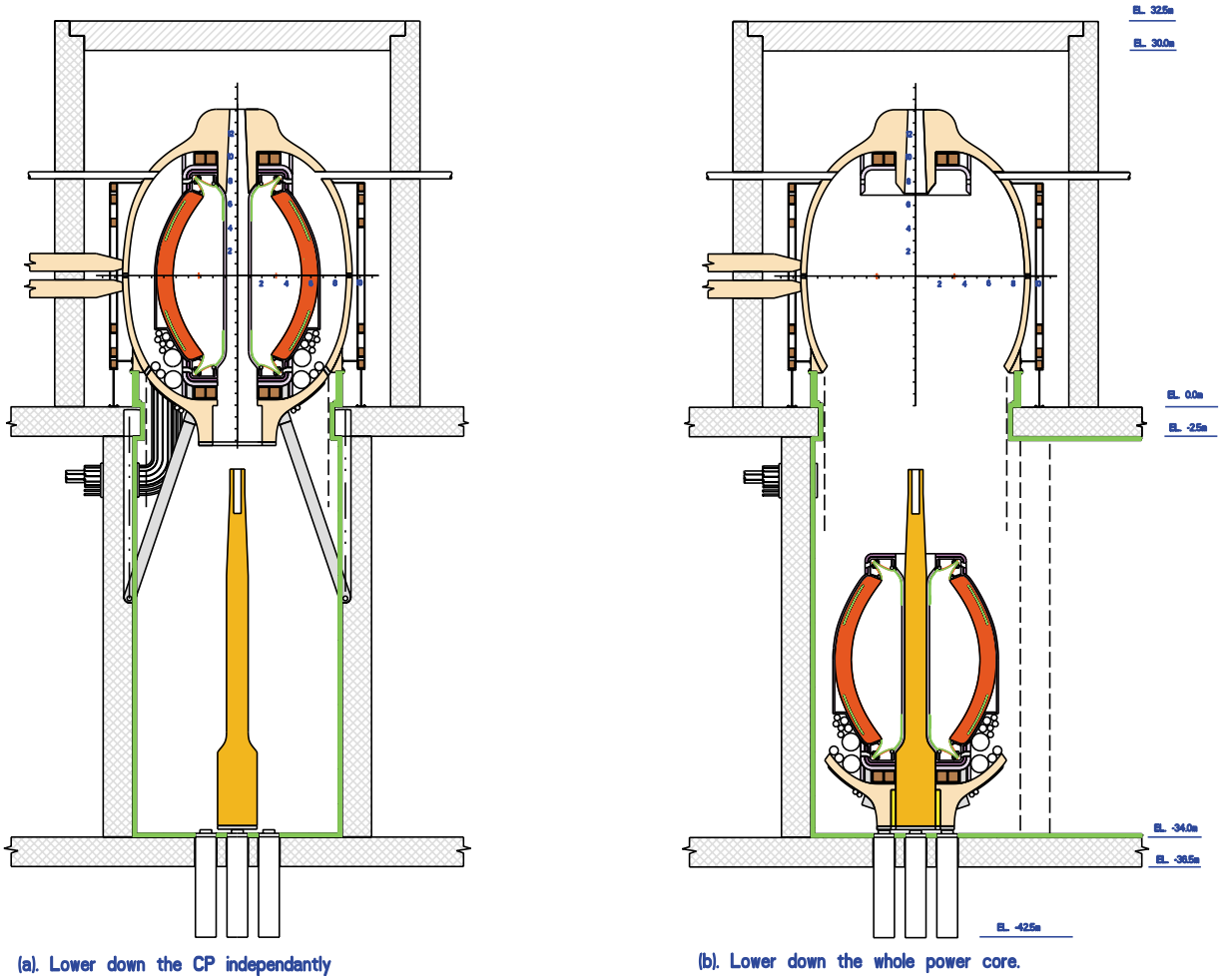

Fig. 6. Paths for centerpost removal.

core assembly, including the first wall, blanket, inboard shield, divertors, and lower PF coils. The lower section is in turn supported by removable supports from below. The upper section extends from the centerpost to the outboard midplane. At the outboard midplane, there is a joint between the upper section and middle section. The upper and middle sections are bolted together with an electrically insulating material in between. A bellows-type connection (with an insulating break) on the inside of the outer shell provides the vacuum barrier across the joint. The TF leads connect to the upper and middle sections at eight equally spaced toroidal locations.

The middle section of the outer shell is connected to the lower section at approximately the same elevation as the lower divertor. At this elevation, the major radius of the joint is adequate to permit vertical removal of the power core. This joint provides the electrical continuity between the middle and lower sections. For removal of the bottom section of the outer shell and power core, the bellows connection is cut and the joint unbolted. The connections between the centerpost

and upper section of the outer shell must also be undone. The middle section of the outer shell is supported off the floor of the test cell. These supports bear the gravity loads of the middle and upper sections of the outer shell, the centerpost, and the upper PF coils attached to the outer shell.

When fully assembled, the outer shell provides a continuous shell that is effective in reacting both in-plane and out-of-plane electromagnetic loads. In additional to the centerpost, penetrations will be required for helium cooling in the power core, the Li–Pb breeding material, vacuum pumping, neutral beam injection, and PF coil services. Some diagnostic penetrations are also likely to be required. Vacuum seals and electrical isolation will be provided at all these locations.

ARIES-ST features a set of five pairs of PF coils located symmetrically about the horizontal midplane, as shown in Fig. 7. The PF coils are supported by the outer shell or shield. The coil supports permit relative motion radially but not vertically. Thus, only gravity and vertical electromagnetic loads are transmitted through the PF coil supports.

3.2. TF power system design

In order to minimize Joule losses in the leads, the TF power supplies have to be located as close to the TF coils as possible. A cylindrical biological shield is provided at a major radius of approximately 13 m. The concrete shield is greater than 2-m thick. The TF power supplies are located just outside this shield.

The large conductor current (34 MA) in the single turn configuration, while formidable, does not appear intractable from a power supply standpoint. One possible scheme for providing a high current power supply has been developed. The overall configuration is depicted in Fig. 8.

Power is taken from a high voltage bus. During the charging of the load, power is fed through a step down transformer such that, after additional step down through converter transformers and DC rectification, the required DC charging voltage is obtained. After charging, an AC bus transfer takes place such that the charging transformer is excluded and the holding transformer is included. The holding transformer ratio is such that the required DC holding voltage is obtained. Additional features could be included to regulate the AC voltage applied to the converter transformers, and hence, the DC voltage, if required, rather than provide two discrete levels. Or, a single step down transformer could be used and additional regulation features could be included to cover the range of required DC voltage.

A large number of diode rectifiers are connected in parallel to provide current to the load. The basic rectifier unit is shown in Fig. 9. It is based on a 6-pulse midpoint topology with interphase reactor. This topology is commonly used for high current rectifiers. It is preferred because there is only one diode in series with the load current (and therefore only one diode voltage drop), and the diode conduction duty is 120° (1/3 of a cycle). By adjusting the phase shifting of the converter transformers, 12- and 24-pulse behavior of the parallel connected groups of converters can be obtained to reduce AC and DC side harmonics.

Current limiting reactors (CLRs) and explosively actuated (pyro) fuses are connected in series with groups of the basic rectifier units as depicted in Fig. 8. The purpose of the CLR is to limit the rate of rise of fault current fed into any one rectifier group in case it suffers a short circuit. The purpose of the pyro fuse is to isolate the faulty rectifier group. In practice, the CLR may not be required as a discrete component; rather the inductance of the bus bar system may be tailored to provide the needed inductance. It may be possible to use a conventional type of fuse instead of a pyro fuse, but this requires more design development and study. The voltage is low and the clearing time (as will be described further on herein) is not unusually short. However, the duty would be DC, which could be problematic.

The best location for inductance and fuses needs to be evaluated by further design development and study. Considering that the bus bar system would consist of a radial tree structure starting with 8 parallel branches and ending in thousands, there are many opportunities for placement and many issues to consider.

The use of a modern large device (Powerex RBS8) was evaluated as a possible commercial

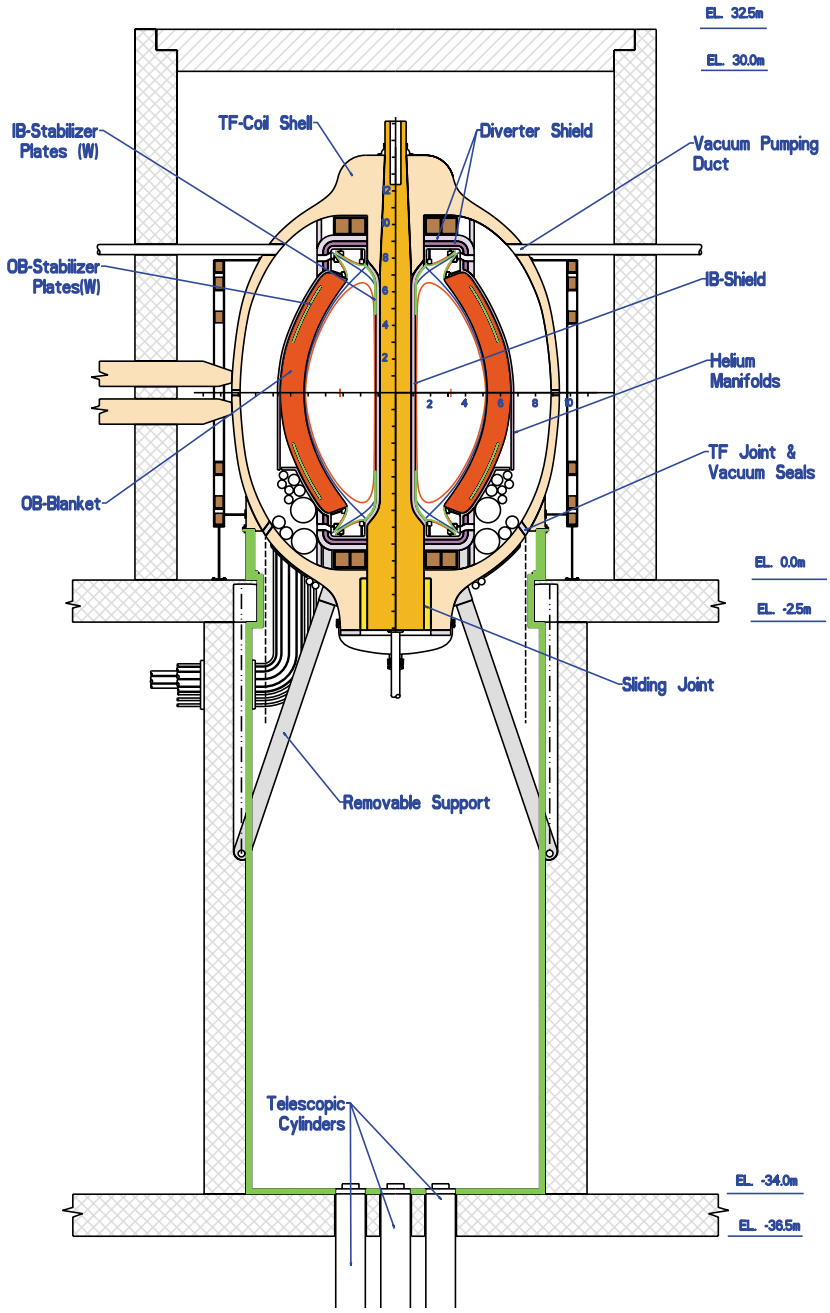

Fig. 7. TF coil system elevation view.

diode for this type of application. Voltage drop characteristics from the data sheet were fit to a curve as shown in Fig. 10. An average diode current of 3 kA was selected so as to produce a reasonable operating temperature (126 °C is less than the maximum temperature of 150 °C for a diode) considering the conduction duty (1/3 cycle), power dissipation, and likely heat sink characteristics. Diode voltage drop at peak 3-pulse bridge current (9 kA) is roughly 1.0 V. This would be the

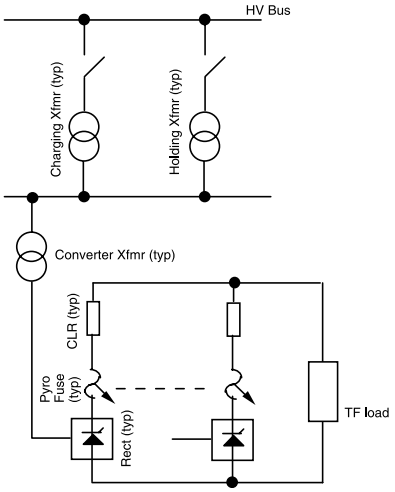

Fig. 8. Overall power supply scheme.

resistive voltage drop across the bridge. Assuming typical characteristics of the AC source impedance, short circuit current of each 6-p bridge would be roughly 5 times rated current, $5 \times 9 \times 2 = 90$ kA.

With a 34.3 MA load, the total number of diodes required would be 11 400. If only one diode path was included in each rectifier bridge leg then the total number of 6-p bridges (3-p pairs) would be 1900. For comparison, the TFTR power supply system uses 7488 thyristors. So, the number of diodes required here is 50% more, but the diodes are much simpler passive devices compared to thyristors.

Total losses in the diodes are on the order of 34 MW. Total prospective short circuit current from the power supply is $5 \times 34 = 170$ MA. Clearly the bus bar layout and physical separation must be designed to absolutely prevent a short circuit, with the level of criticality increasing as one moves through the radial branches of the tree toward the final connection to the load.

In case a diode suffers a short circuit, it must be isolated by the pyro fuse, and it is important that the I^2t be limited to a value such that the diode does not rupture (explode). For the selected diode, this value is 1.5×10^7 A^2 s. Assuming the power supply produces 10 VDC, a 1 μH inductance between the faulty diode and all of the other power supply feeding it would be sufficient to limit the rate of rise of current such that more than 5 ms would be available to achieve the isolation prior to reaching the limiting I^2t. This should be adequate to sense and interrupt. Probably, the sensing would be based on dI/dt being abnormally high in such a case. Also, the maximum current would be less than the inherent short circuit current of the bridge (mentioned earlier) for which it would have to be braced in any case.

There may be opportunities for reducing the losses in the diodes, and for using fewer diodes, by immersing them in LN_2.

4. System performance

4.1. Electrical characteristics

Electrically, the TF system has only a single turn. A current of 34.3 MA is required to satisfy

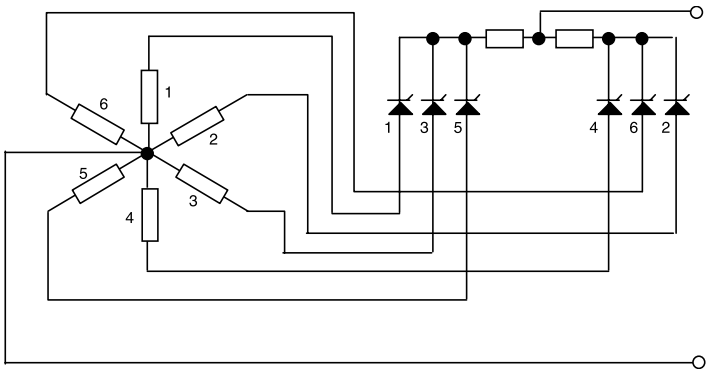

Fig. 9. Six-pulse midpoint converter with interphase reactor.

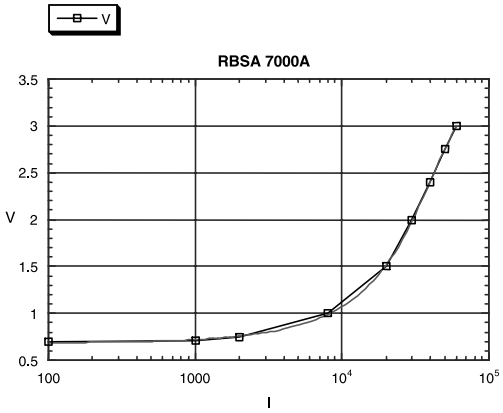

Fig. 10. Diode voltage drop characteristics.

the TF requirement of 2.14 T at 3.2 m. The voltage drop across the TF coil system is 8.5 V, corresponding to Joule losses of 291 MW. The Joule losses occur predominantly in the centerpost (242 MW) with the balance occurring in the outer shell (31 MW) and bus (19 MW). The current density in the centerpost conductor at the midplane is 1.47 kA/cm^2. The electrical resistivity of CuCrZr is 80% IACS and varies with temperature as shown in Fig. 1.

The outer shell is constructed of a 5000 series aluminum alloy. This class of conductor was chosen because the outer shell can be fabricated using a spray casting technique. There are alloys in this series that exhibit good electrical conductivity (~ 3.7 $\mu\Omega$ cm) and weldability. The outer shell thickness is approximately 0.7 m. This thickness results in low stresses, low current density in the outer shell (0.07 kA/cm^2), and low Joule losses (31 MW).

A feature of this configuration concept is the sliding joint that provides electrical continuity between the bottom section of the centerpost and the lower section of the outer shell. The sliding joint is located at a radius of 1.6 m and has a height of 3.6 m. The sliding joint concept is patterned after C-Mod and MAST, utilizing Feltmetal pads. One key design criterion for the joint is the current density. Guidance received from the MAST project [10] based on their testing was to keep the current density in the Feltmetal pads below 1 kA/cm^2 for steady state applications. At a radius of 1.6 m, it should be possible to fit 200 joints (with 2 pads per joint) around the circumference of the interface. Because the sliding joint is located near a sharp corner, the current distribution is peaked near the corner with a 4:1 peaking factor. Nevertheless, the peak current density in the Feltmetal pads is an acceptable 0.8 kA/cm^2.

The stored energy in the TF coil system is 6.2 GJ. In the event of a LOCA incident during which all coolant flow to the TF was lost, the temperature rise in the centerpost would be a modest 32 °C due to dissipation of the stored energy. For prolonged periods without any cooling in the centerpost, the temperature rise due to the afterheat in the centerpost needs to be considered. The calculated peak temperature of 1018 °C should not be large enough to jeopardize plant safety by volatilizing activated particulates. However, the temperature excursion in the centerpost might well put the capital investment at risk. For this reason, provisions for auxiliary cooling of the centerpost for removal of the modest afterheat (≈ 2 kW maximum) should be made.

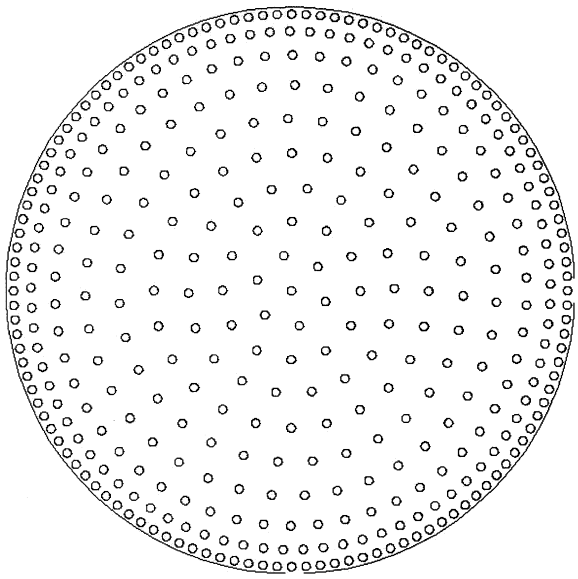

Fig. 11. TF centerpost cross-section view.

4.2. Thermal–hydraulic performance

The centerpost is cooled with water with a 30 °C inlet temperature, slightly above ambient temperature. The water is fed in at the top and exits at the bottom. The feed on top was chosen to minimize thermal stresses across the contact interface between the centerpost and outer shell. The top plenum feeds 386 individual circular cooling passages that are collected in a plenum at the bottom. Each cooling passage has a diameter of approximately 2.6 cm with an average spacing of 9.2 cm. A cross-section view of the TF centerpost at the midplane is shown in Fig. 11. The coolant holes are more closely spaced towards the plasma because that is where the nuclear heating is localized. The coolant fraction is approximately 8.3% at the midplane of the centerpost.

The heat load to be removed from the centerpost during initial operation is approximately 406 MW, consisting of 242 MW of Joule heating and 164 MW of nuclear heating. The coolant velocity was limited to 10 m/s to avoid excessive erosion. The required flow rate is 2155 kg/s with an outlet temperature of 75 °C. To achieve this flow rate, the required inlet pressure is a modest 1.36 MPa with an outlet pressure of 0.15 MPa. The average conductor temperature at the midplane is approximately 33 °C higher than the bulk temperature of the coolant due to an 18 °C film temperature rise and a 15 °C temperature rise across the conductor. The Joule heating in the centerpost increases by 33 MW after 3 FPY. With the same flow rate, the outlet temperature increases by 4–79 °C.

The heat load to be removed from the outer shell is low (70 MW) [2]. Nuclear heat loads in the outer shell are ~21 MW in the lightly shielded collar and only 18 MW elsewhere. The 70 MW total heat load is removed by water flowing through stainless steel tubes embedded in the spray cast outer shell.

4.3. Structural analysis

A preliminary structural analysis of the ARIES-ST TF coil system was performed using the ANSYS code. ANSYS is a convenient choice because the code calculates the current distribution in the TF coil, the resulting electromagnetic loads, and the associated stress distribution as part of one package. The ANSYS model included the PF coils and plasma in its calculation. The PF coils and plasma cause out-of-plane (toroidal) forces in the TF centerpost and outer shell due to interactions between their poloidal fields and the TF current. In addition, vertical loads on the PF coils attached to the outer shell produce mechanical loads on the TF outer shell at the point of attachment.

Two options for supporting the centerpost were explored:

1) Let the centerpost be free to expand vertically and radially at the bottom where the centerpost penetrates the outer shell. No relative torsional displacements would be permitted.
2) Tie the centerpost to the outer shell at the bottom, allowing no relative vertical or torsional displacements. Relative radial displacements would still be permitted.

The first option was chosen as the baseline because it is the simplest and it appears to work acceptably well. Thermal growth of the centerpost is not an issue because the centerpost is not vertically constrained. In the second option, the thermal growth is vertically constrained. This feature might actually prove advantageous and make the second option more attractive than the first. It would reduce the peak VonMises stress in the centerpost, put the centerpost in a state of triaxial compression, increase the contact pressure across the joint between the centerpost and outer shell at the top, and would have no relative vertical displacement at the bottom to complicate the sliding joint design and cooling connections to the centerpost.

The centerpost is subject to radial, compressive loads due to the vertical TF current crossing the TF. These radial loads result in stresses in the toroidal direction, i.e., hoop stresses, that range from 16 MPa (compression) at the outer surface to 60 MPa (compression) in the center, as shown in Fig. 12. In addition, there is a vertical separating force on the centerpost due to radial currents near the ends of the centerpost crossing the TF. Because the diameter of the centerpost is larger at the

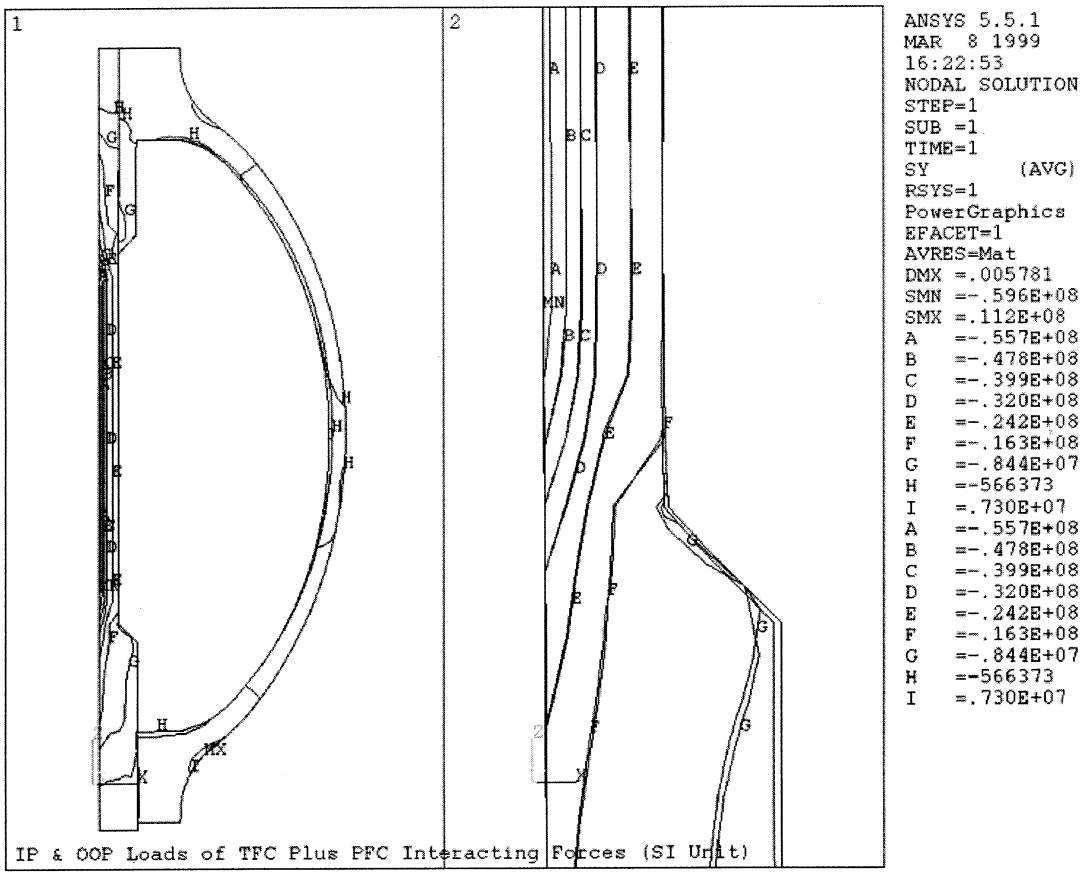

Fig. 12. TF coil hoop stress contours.

bottom than at the top, there is also a net downward vertical force on the centerpost. The net vertical load is reacted where the centerpost is attached to the outer shell at the top. Sufficient preload must be provided at this attachment to maintain adequate contact pressure across the joint, which provides electrical continuity between the centerpost and outer shell.

In the first option, the centerpost is free to expand vertically. Vertical forces on the centerpost result in axial tensile stresses ranging from 24 MPa (tension) in the center to 46 MPa (tension) at the outer surface of the centerpost, as shown in Fig. 13. Note that the axial stresses are smaller in magnitude and opposite in sign to the hoop stresses. Note also that they peak on the outer surface whereas the hoop stresses peak in the center. The VonMises stress in the centerpost is fairly uniform along its length, ranging from 55 MPa at the outer surface to 76 MPa in the center, as shown in Fig. 14. Stresses in the outer shell are low everywhere, with a VonMises stress less than 21 MPa except in a very local region near the corner by the collar where the stresses are less than 30 MPa.

The continuous outer shell is ideal for resisting both in-plane and out-of-plane loads. The absence of turn-to-turn insulation in a single turn coil design removes the traditional weak link for stresses arising from out-of-plane loads. The only electrical insulation is at the outboard midplane. Interlaminar shear stresses are very low in this

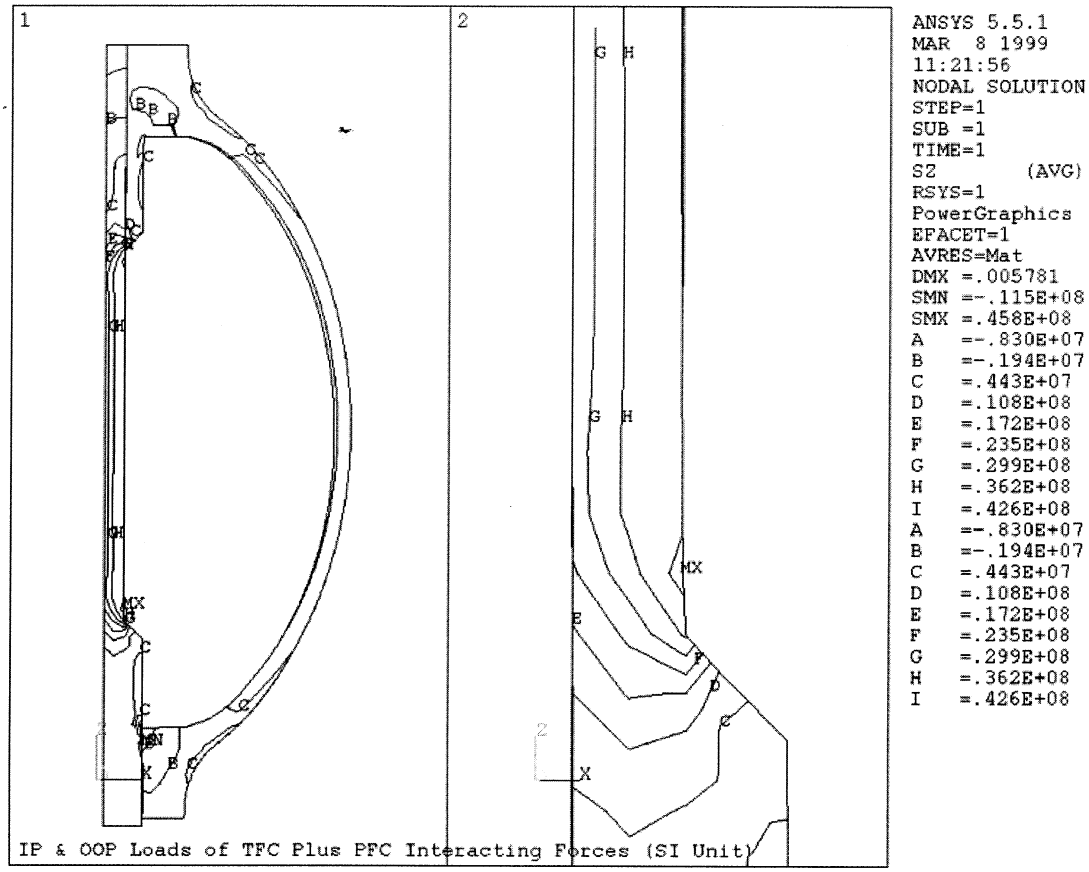

Fig. 13. TF coil axial stress contours.

region, less than 4 MPa. More detailed design and analysis are required to quantify stresses due to out-of-plane loads where the centerpost interfaces with the outer shell at the top and bottom.

In the second option, the bottom of the centerpost is tied to the outer shell, so it is not free to expand vertically. This does not substantially change the stresses due to EM loads. However, there is a substantial change in thermal stresses. The only element that has a substantial temperature gradient is the centerpost. The inlet temperature for the coolant is nominally 30 °C at the top with an outlet temperature of 75 °C at the bottom. Temperature differences across the outer shell are small because of the shorter coolant path lengths and much lower current density. The centerpost tends to grow thermally whereas the outer shell does not. However, in the second option, the axial displacements at the bottom are forced to be equal. This causes an axial thermal stress in the centerpost of 38 MPa (compression). Because the axial thermal stress is opposite in sign to the axial stress arising from the EM loads, the peak axial stress in the center of the centerpost changes from approximately 46 MPa (tension) in the first option to 20 MPa (compression) in the second option. This reduces the peak Von-Mises stress from 76 to 44 MPa. In the second option, the centerpost is in a state of tri-axial compression.

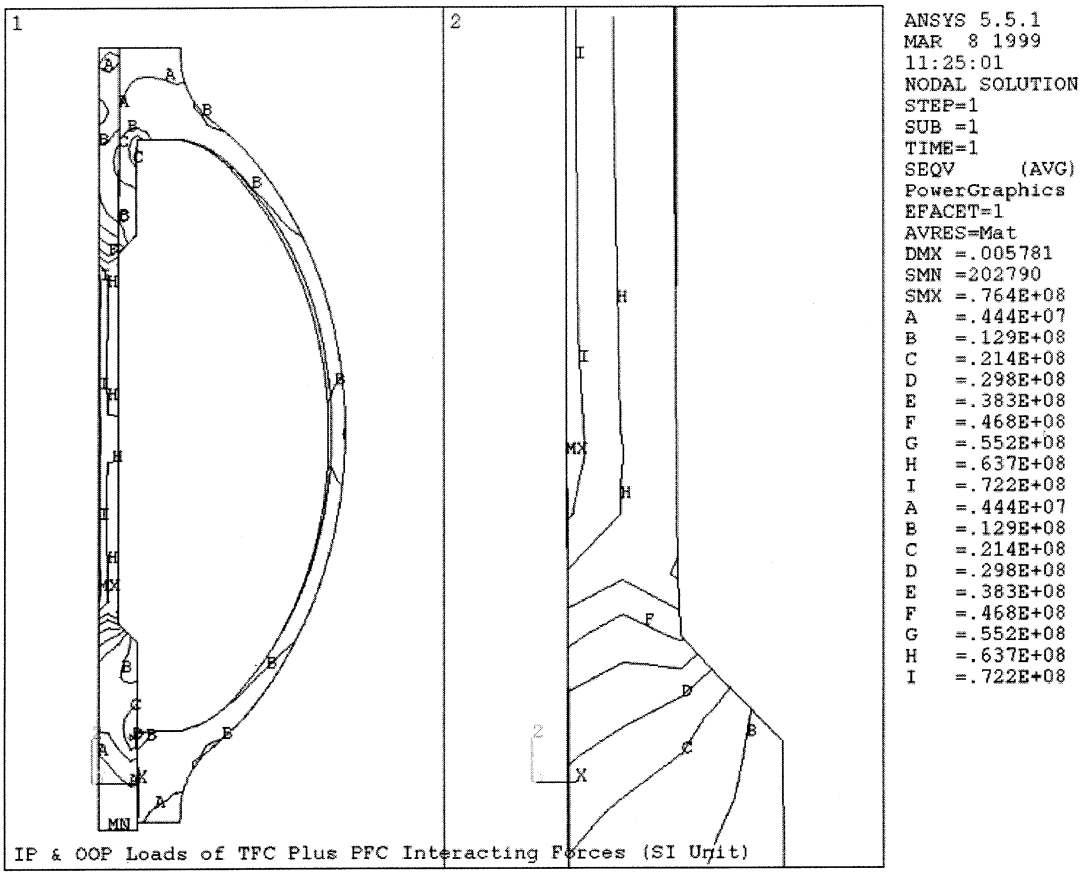

Fig. 14. TF coil VonMises stress contours.

The development of structural design criteria for fusion materials and applications has been an ongoing activity for the past two decades. Recent work has been done under the auspices of the ITER project. For calculating allowable stresses in the ARIES-ST design, the ITER criteria [11] were followed. In general, for structural materials, the design Tresca stress value, S_m, at design temperatures less than 500 K shall be the lower of 2/3 S_y (yield strength) or 1/2 S_u (ultimate tensile strength) as long as the reduction of area at fracture is greater than 40%. For materials where this is not satisfied, a lower allowable stress limit should be considered in view of possible brittle behavior. A suggested guideline is a more conservative value of S_m set at 1/2 S_y. Based on elastic analysis, the stress limits are:

- 1.0 KS_m for primary membrane stresses
- 1.3 KS_m for primary membrane plus bending stresses
- 1.5 KS_m for primary plus secondary stresses

The appropriate K values in the base metal for various load combination categories are

- For normal operating conditions, $K = 1.0$
- For anticipated conditions, $K = 1.1$
- For unlikely conditions, $K = 1.2$; evaluation of secondary stress not required
- For extremely unlikely conditions, $K = 1.3$; evaluation of secondary stress not required

Clearly, at least in the outer half of the centerpost (at a radius greater than 0.5 m), the material will be embrittled within 3 FPY. For primary

membrane stresses under normal operating conditions, the allowable stress would be 1/2 S_y. High strength, high conductivity copper alloys tend to radiation harden in this temperature range. For conservatism, we assumed unirradiated strength properties. A wide range of strength properties is quoted in the literature for CuCrZr, depending on the thermo-mechanical history of the material. For calculating the allowable stress in the centerpost, we assumed a yield strength of 350 MPa, which is consistent with the maximum yield strength that might be expected following a welding or brazing operation [5]. The allowable primary membrane stress would be 175 MPa. The peak VonMises stress (which approximates the Tresca stress) in the first option is 76 MPa or 43% of the allowable primary membrane stress. The peak VonMises stress in the second option is 44 MPa or 25% of the allowable primary membrane stress. Thus, it does not appear that primary stresses will be limiting.

Based on the ITER criteria, no stress (primary plus secondary) can exceed 1.5 KS_m. For normal operation, the allowable stress for this combination of stresses in the centerpost would be 3/4 S_y or 262 MPa. Stress concentrations around cooling holes in the range of 2–3 can be expected. This would result in a hoop stress of 120–180 MPa (compression) around the cooling holes in the center of the centerpost, rather than the average value of 60 MPa (compression). Thermal stresses can also be expected due to temperature gradients around the cooling holes. The magnitude of these stresses is estimated to range from 33 MPa (tension) around the cooling holes to 15 MPa (compression) away from the cooling holes. Note that the thermal stress is opposite in sign to the hoop stresses that peak around the cooling holes, thereby offsetting their impact. More detailed design and analysis and better material property data for laser formed conductor are required to make definitive judgements about the acceptability of the stresses for the TF coil design. However, these increments appear small relative to the margin between the allowable stress of 262 MPa and the calculated primary membrane stress values of 76 and 43 MPa for the first and second options, respectively. Therefore, it appears promising that adequate structural margin exists for the ARIES-ST TF coil system design.

5. Conclusions

The ARIES-ST TF design is based on a single turn construction consisting of a stepped cylindrical centerpost along the major axis and a toroidally continuous outer shell. High strength, high conductivity copper alloys operating at low temperatures (between room temperature and 100 °C) appear to be interesting candidates for use in the centerpost. Irradiation in this temperature range causes radiation hardening and embrittlement. However, stresses in the centerpost appear low enough to satisfy brittle material allowables. Swelling and creep are not issues at these low temperatures and stresses. The key consideration in selecting the copper alloy to be used in the centerpost may be the fabrication method. Using the laser forming technique identified by Boeing for fabricating the centerpost strongly favors a PH alloy such as CuCrZr over a DS alloy such as Glidcop AL-15. The outer shell is fabricated with a high conductivity aluminum alloy using a spray casting technique.

The centerpost and outer shell are both water-cooled with an inlet temperature appropriate for ambient heat removal, nominally 30 °C. Trade studies were conducted to assess other options for cooling, ranging from gaseous helium at 10 K to liquid lithium at 200 °C. None of these options appeared superior to ambient water cooling based on expected thermodynamic efficiencies or design simplicity.

The centerpost lifetime appears to be limited by economic considerations. For ARIES-ST, disposal of the centerpost as Class C waste requires replacement every 6 FPY (using Fetter limits), which is every second replacement of the ferritic steel structures facing the plasma. Transmutations will result in an increase in Joule losses of approximately 12.5% after 3 FPY. Because the centerpost is relatively inexpensive (< \$7M), economic considerations appear to favor replacement

more frequently, i.e., concurrent with every replacement of the ferritic steel structures facing the plasma. The TF coil system is designed to be compatible with vertical maintenance from below. The centerpost can be removed separately or as part of the power core assembly. The outer shell is divided into three segments. The upper and middle segments are permanent structures, designed for the life of the plant and not removed with the power core assembly. The lower segment of the outer shell provides support for the power core assembly and although designed for the life of the plant, is removed for replacement of the power core assembly. The TF coil system provides the primary vacuum boundary for the plasma and for superconducting PF coils inside the outer shell. Vacuum seals are provided at all penetrations.

The TF coil system is powered by a high current (34 MA), low voltage (8.5 V across the TF leads) power supply. Joule losses in the system are 291 MW, predominantly in the centerpost. Because of the high current, large bus cross-sections are required to keep the Joule losses in the bus low. The power supply must be located as close to the TF coil system as possible.

The TF coil system design addresses a number of the concerns (complexity) and criticisms (high cost, high recirculating power) of fusion. It does this by:

- Applying advanced, but available laser forming and spray casting techniques for manufacturing the TF coil system.
- Adopting a simplified single TF coil system to make assembly and maintenance much easier. The single turn design also avoids the necessity of using the insulation as a structural component of the TF coils, and hence, is much more robust than multi-turn designs.
- Using high conductivity copper and modest current densities to keep the recirculating power modest.

References

[1] S.A. Fabritsiev, S.J. Zinkle, B.N. Singh, Evaluation of copper alloys for fusion reactor divertor and first wall components, J. Nucl. Mater. (1996).
[2] L. El-Guebaly, ARIES Team, ARIES-ST Nuclear Analysis and Shield Design, Fusion Eng. Des., in press.
[3] S.A. Fabritsiev, A.S. Pokrovsky, S.J. Zinkle, D.J. Edwards, Low temperature embrittlement of copper alloys, J. Nucl. Mater. September (1996).
[4] H.Y. Khater, E.A. Mogahed, D.K. Sze, et al., ARIES Team, ARIES-ST Safety Design and Analysis, Fusion Eng. Des., in press.
[5] S.J. Zinkle, S.A. Fabritsiev, Final Report to US Home Team for 1994 ITER R&D Task T7: Assessment of Copper Alloys for High Heat Flux Applications.
[6] L.M. Waganer, D.A. Deuser, K.T. Slattery, et al., Ultra-Low Cost Coil Fabrication Approach for ARIES-ST, Fusion Eng. Des., in press.
[7] M.C. Billone, Materials Input for the ARIES-ST Design Program, in: Fusion Materials Semiannual Progress Report for the Period Ending December 1998, US Department of Energy report DOE/ER-0313/24, 1999.
[8] F. Puhn, et al., Mechanical Design of a High-Beta TFCX Tokamak with a Demountable TF Coil, in: Proceedings of 13th Symposium on Fusion Technology (SOFT), Varese, Italy, September, 1984.
[9] Holt Murray, High Current Density, Cryogenically Cooled Sliding Electrical Joint Development, PPPL-2370, September, 1986.
[10] G. Voss, Culham Laboratorties, United Kingdom, private communication, 1999.
[11] ITER Design Criteria, June 1, 1995.
[12] D.J. Alexander, S.J. Zinkle, A.F. Rowcliffe, Fracture Toughness of Copper-Base Alloys for ITER Applications, in: Fusion Materials Semiannual Progress Report for the Period Ending December 1998, US Department of Energy report DOE/ER-0313/24, 1999.
[13] J.W. Davis (Ed.), ITER Material Properties Handbook, ITER Doc. S74-RE-1-97-08-01 W1.5, August, 1997.